

Eclipsing Binaries as Astrophysical Laboratories: Internal Structure, Core Convection and Evolution of the B-star Components of V380 Cygni

Edward F. Guinan¹, Ignasi Ribas^{1,2}, Edward L. Fitzpatrick¹, Álvaro Giménez^{3,4}, Carme Jordi², George P. McCook¹, and Daniel M. Popper^{5,6}

ABSTRACT

New photometric solutions have been carried out on the important eccentric eclipsing system V380 Cygni (B1.5 II-III + B2 V) from *UBV* differential photoelectric photometry obtained by us. The photometric elements obtained from the analysis of the light curves have been combined with the spectroscopic solution recently published by Popper & Guinan and have led to the physical properties of the system components. The effective temperature of the stars has been determined by fitting IUE UV spectrophotometry to Kurucz model atmospheres and compared with other determinations from broad-band and intermediate-band standard photometry. The values of mass, absolute radius, and effective temperature, for the primary and secondary stars are: $11.1 \pm 0.5 M_{\odot}$, $14.7 \pm 0.2 R_{\odot}$, $21\,350 \pm 400$ K, and $6.95 \pm 0.25 M_{\odot}$, $3.74 \pm 0.07 R_{\odot}$, $20\,500 \pm 500$ K, respectively. In addition, a re-determination of the system's apsidal motion rate has been done from the analysis of 12 eclipse timings obtained from 1923 to 1995. The apsidal motion study yields the internal mass distribution of the more luminous component. Using stellar structure and evolutionary models with modern input physics, tests on the extent of convection in the core of the more massive B1.5 II-III star of the system have been carried out. Both the analysis of the $\log g - \log T_{\text{eff}}$ diagram and the apsidal motion study indicate a star with a larger convective core, and thus more centrally condensed, than currently assumed. This has been quantified in form of an overshooting parameter with a value of $\alpha_{\text{ov}} \approx 0.6 \pm 0.1$. Finally, the tidal evolution of the system (synchronization and circularization times) has also been studied.

Subject headings: stars: fundamental parameters — binaries: eclipsing — stars: evolution — stars: early-type — stars: individual (V380 Cyg)

1. Introduction

The bright eclipsing binary V380 Cyg (HR 7567; HD 187879; HIP 97634; $V_{\text{max}} = 5.68$; $P = 12.426$ days; B1.5 II-III + B2 V; Hill & Batten 1984) has properties that make it an important “astrophysical laboratory” for studying the structure and evolution of massive stars. In particular, the extent of convection in the stellar core and the internal mass distribution of the primary component can be probed because the system has an eccentric orbit with a well-established apsidal motion rate. Also, V380 Cyg can provide independent measures of the initial fractional helium abundance of the system (Y), which is an

¹Department of Astronomy & Astrophysics, Villanova University, Villanova, PA 19085, USA. E-mail: edward.guinan@villanova.edu, iribas@ast.villanova.edu, fitz@ast.villanova.edu, george.mccook@villanova.edu

²Departament d'Astronomia i Meteorologia, Universitat de Barcelona, Av. Diagonal, 647, E-08028 Barcelona, Spain. E-mail: carme@am.ub.es

³Laboratorio de Astrofísica Espacial y Física Fundamental, Apartado 50727, E-28080 Madrid, Spain. E-mail: ag@laeff.esa.es

⁴Instituto de Astrofísica de Andalucía, CSIC, Apartado 3004, E-18080 Granada, Spain

⁵Division of Astronomy and Astrophysics, UCLA, CA 90095-1562, USA

⁶Deceased

important and fundamental quantity but empirically difficult to measure. Accurate fundamental physical properties of the components (e.g., mass, radius, effective temperature, etc.) are however required to carry out such analyses.

V380 Cyg consists of an evolved, more massive, and more luminous primary component and a main sequence secondary star. It has an eccentric orbit ($e = 0.23$) and an orbital period of 12.426 days. Several spectroscopic studies have been carried out to determine its orbital properties and the masses, temperatures, and luminosities of the component stars (see Batten 1962; Popper 1981; Hill & Batten 1984; Lyubimkov et al. 1996). The first light curve of the system by Kron (1935), as well as the more modern photometry by Semeniuk (1968) and Battistini, Bonifazi, & Guarnieri (1974), revealed shallow eclipses with depths of ~ 0.12 mag and ~ 0.09 mag for primary and secondary minima, respectively. Moreover, these photometric measurements show that the secondary eclipse is displaced from $0^{\circ}5$, indicating an eccentric orbit, while changes in the displacement between primary and secondary minima indicate the presence of apsidal motion with a period of about 1500 yrs.

As discussed by Giménez (1984) and Giménez, Claret, & Guinan (1994), V380 Cyg is an ideal binary system for the study of convective overshooting in the cores of massive stars because of the evolutionary stages of its component stars. Because of the eccentric orbit and the eclipsing nature of the binary, it is possible to determine the apsidal motion rate. From this, additional constraints on the internal mass distribution and the evolutionary state of an evolved massive star also can be established.

Because V380 Cyg provides potentially important tests of stellar structure and evolution, we have carried out new high signal-to-noise spectroscopic and photometric observations of the system and performed a new, detailed investigation of its properties. In §2 we present the new observations. The effective temperature determination, based on both standard photometry and UV/optical spectrophotometry, is discussed in §3. In §4 we concentrate on the analysis of the light curves. §5 is devoted to the study of eclipse timings, leading to an accurate determination of the apsidal motion rate. The properties of the system components

are compared with the predictions of theoretical models in §6. The tidal evolution of the system (circularization and synchronization times) is analyzed in §7. Finally, the main conclusions of our study are presented in §8.

2. Observational Data

New high-quality spectroscopic and photometric observations have been collected for V380 Cyg. The following sections contain a brief description of these data.

2.1. Spectroscopy

V380 Cyg is difficult to resolve spectroscopically into a double-line binary because of the large luminosity difference between the component stars. Therefore, very high signal-to-noise and high-resolution spectroscopic observations are needed to measure the radial velocity shifts of the faint lines of the secondary star. Such high signal-to-noise and high-resolution spectroscopy was recently secured by us and led to a new, accurate radial velocity curve, which was carefully analyzed in a previous paper (Popper & Guinan 1998; hereafter Paper I). The spectroscopic solution obtained in Paper I (basically velocity semi-amplitudes and systemic velocity) has been adopted in the present study.

2.2. Photometry

UBV differential photoelectric photometry of V380 Cyg was carried out from 1988 to 1997 using robotic, automatic photoelectric telescopes (APTs) located on Mt. Hopkins, Arizona. From 1988 to 1989 the photometry was conducted with the Phoenix-10 APT telescope, a 25-cm robotic telescope equipped with a 1-P21 photometer and filters matched to the standard *UBV* system. During 1995–1997 the photometry was conducted using the Four College Consortium (FCC) 0.8-m APT. The FCC APT is equipped with filters closely matching the standard *UBV* system and a refrigerated Hamamatsu photoelectric detector. Differential photometry was obtained in which HD 189178 (B5 V, $V = 5.47$) was employed as the comparison star, while HD 188892 (B5 IV, $V = 4.94$) served as the check star. No evidence of significant light variations (down to the few milimagnitude level) was found for the comparison–check

star sets. The observations were reduced using photometric reduction programs at Villanova University. Differential extinction corrections were applied, but these corrections were typically very small since the comparison star is within 2 deg. of V380 Cyg and the stars were never observed at high air mass. The photometric measurements are listed in Table 1.

U, *B*, and *V* differential light curves are shown in Figure 1. We adopted the following ephemeris for computing the orbital phase: $T_{\text{MinI}} = \text{HJD}2441256.544 + 12.425719E$ (see §5). As can be seen in the plots, the shallow secondary minimum occurs at 0°403. Also, the light curves show out-of-eclipse brightness variations with maximum light occurring near 0°15. The displacement of the secondary eclipse from phase 0.5, as noted in §1 above, is caused by the eccentric orbit of the system, while the outside eclipse light variations arise primarily from the changing tidal distortion, chiefly from the larger star as it moves in the eccentric orbit. According to the recent spectroscopic solution of Paper I, periastron passage occurs near 0°15 where the stars reach their greatest tidal deformations.

3. Temperature Determination

A complete analysis of the V380 Cyg system requires precise measurements of the stellar effective temperatures (T_{eff}). For this purpose, we explored the use of published T_{eff} vs. intrinsic color calibrations — utilizing several different photometric systems — and also we performed a detailed study of the shape of the UV/optical stellar energy distribution. Both these methods for determining effective temperatures are discussed below.

Intermediate-band Strömgren and Vilnius photometric indices for V380 Cyg are available from the literature and are listed in Table 2 along with our new measurements in the Johnson *UBV* system. The Johnson photometry was secured out-of-eclipse, when both stars were fully visible. The phases at which the Strömgren and Vilnius measurements were made is not known, although this is not likely to be a critical problem for V380 Cyg because the secondary component is much less luminous than the primary component and the temperatures and color indices of the two stars are similar. A summary of the reddening and T_{eff} re-

sults for the three photometric systems is given in Table 2. An *a priori* estimate of the expected uncertainties in these results is difficult, but clearly depends on both random errors in the stellar photometry and systematic errors in the various calibrations themselves. It is clear, however, that the level of agreement among the various systems is unsatisfactory, with a range of over 4000 K and a standard deviation of ~ 1800 K — nearly 10% of the value of T_{eff} itself.

In view of the discrepancies among the photometric results for T_{eff} , we employed a different technique for determining this important quantity. We modeled the observed shape of the UV/optical energy distribution of V380 Cyg using theoretical spectra generated with the Kurucz's *ATLAS9* model atmosphere program. This analysis was developed by Fitzpatrick & Massa (1999; hereafter FM99) and has been applied previously to an eclipsing binary system by Guinan et al. (1998).

For a binary system, the observed energy distribution depends on the surface fluxes of the binary's components and on the attenuating effects of distance and interstellar extinction. This relationship can be expressed as:

$$f_{\lambda \oplus} = \left(\frac{R_P}{d} \right)^2 \left[F_{\lambda}^P + \left(\frac{R_S}{R_P} \right)^2 F_{\lambda}^S \right] \times 10^{-0.4E(B-V)[k(\lambda-V)+R(V)]} \quad (1)$$

where F_{λ}^P and F_{λ}^S are the surface fluxes of the primary (P) and secondary (S) components, R_P and R_S are the absolute radii, and d is the distance to the binary. The last term carries the extinction information, including $E(B-V)$, the normalized extinction curve $k(\lambda-V) \equiv E(\lambda-V)/E(B-V)$, and the ratio of selective-to-total extinction in the *V* band $R(V) \equiv A(V)/E(B-V)$.

The modeling process consists of a non-linear least squares determination of the optimal values of all the parameters which contribute to the right side of equation 1. In principle, the problem can involve solving for two sets of Kurucz model parameters (i.e., one set of T_{eff} , surface gravity, metallicity [m/H], and microturbulence velocity v_{micro} values for each star), the ratios $(R_P/d)^2$ and R_S/R_P , $E(B-V)$, $k(\lambda-V)$, and $R(V)$. For V380 Cyg, however, a number of simplifications can be made: (1) the temperature ratio of the two stars is known from the light curve analysis (see §4 below); (2) the surface gravities are known from the combined result of the light and radial

velocity curve analyses (see §4); (3) $[m/H]$ can be assumed to be identical for both components; (4) v_{micro} can be assumed to be 0 for the much fainter secondary star; (5) the ratio R_S/R_P is known from the light curve analysis (see §4); (6) the properties of normalized UV/optical extinction are constrained by a small number of parameters (Fitzpatrick & Massa 1990; Fitzpatrick 1999); and (7) the standard value of $R(V) = 3.1$ may be assumed, without affecting the T_{eff} determination.

Adopting these simplifications, we modeled the observed UV/optical energy distribution of V380 Cyg by solving for the best-fitting values of T_P , $[m/H]_{\text{PS}}$, v_{micro}^P , $(R_P/d)^2$, $E(B-V)$, and $k(\lambda - V)$. The observational data used in the analysis includes the Johnson and Strömgren optical photometry listed in Table 2 and UV spectrophotometry from the *International Ultraviolet Explorer (IUE)* satellite. The *IUE* data consist of a low-dispersion short-wavelength spectrum (SWP38553; 1150 Å to 1980 Å) and a low-dispersion long-wavelength spectrum (LWP17712; 1980 Å to 3000 Å), both secured out-of-eclipse. These data were obtained from the *IUE* Final Archive and thus were processed using the *NEWSIPS* system (Nichols & Linksy 1996). We utilized the algorithms of Massa & Fitzpatrick (2000) to correct these *NEWSIPS* data for strong thermal and temporal systematics and to place them on the *Hubble Space Telescope* absolute UV/optical calibration system (Bohlin 1996). The final *IUE* spectrum was then re-sampled to match the wavelength binning of the *ATLAS9* models (see FM99). This binned spectrum can be seen in Figure 2 (small filled circles). The presence of the 2175 Å interstellar medium extinction feature is clear, as are the strong stellar absorption features in the 1400 Å, 1500 Å, and 1900 Å regions characteristic of evolved early B-type stars. For display purposes, we also show the Johnson and Strömgren magnitudes, converted to fluxes, in Figure 2 (large filled circles and triangles). However, in the fitting procedure the photometric indices themselves (i.e., V , $B-V$, $U-B$, $b-y$, m_1 , c_1 , β) were compared with synthetic values for the models. The calibration of the synthetic photometry is discussed by FM99 and in a forthcoming paper by E. L. Fitzpatrick & D. Massa (in preparation).

The best-fitting, reddened, and distance-at-

tenuated *ATLAS9* model of V380 Cyg's energy distribution is shown in Figure 2 (histogram-style curve) overplotted on the V380 Cyg observations. In the UV region, the residuals to the fit ("Model – Star") are shown below the energy distribution, with the vertical bars indicating the statistical error in the *IUE* data. The major discrepancies occur near the interstellar Ly α line (1215 Å) and the C IV stellar wind line (1550 Å). These regions were excluded from the fit, as indicated by the crosses over the data points. Several other data points, corresponding to spurious feature in the models were also excluded (see FM99). (Note that the fit appears poorest in the 2000 to 2300 Å region because of the low signal-to-noise level of the data.)

The parameters characterizing the fit are listed in Table 3. The values of T_{eff} and $E(B-V)$ are within the range found from the photometric analysis (see Table 2) but are much more precisely determined. (The synthetic photometry of the best-fitting model reproduces all the Johnson and Strömgren photometric indices to within the expected errors of the data.) The attenuation factor of the energy distribution is also derived from the analysis, and it yields the distance to the system (Table 4) when combined with the absolute radius of the primary component (see Guinan et al. 1998 for further discussion on this issue). The values of $[m/H]$ and v_{micro} bear some comment. FM99 found that in B-type stars with significant stellar winds, correlated increases in the best-fitting values of v_{micro} and decreases in $[m/H]$ occur. These combinations reproduce the observed opacity features very well, but it is likely that neither parameter faithfully represents a corresponding stellar property. This probably arises because the stellar opacity features form in a region with a weak velocity gradient, while the models explicitly assume an atmosphere in hydrostatic equilibrium. (See FM99 for additional discussion.) The implication for this work is that the value of $[m/H]$ derived from this analysis is almost certainly an underestimate of the true metallicity of V380 Cyg. For further analysis, we adopt a metal abundance of $[m/H] = -0.2$ based on recent analyses of nearby B-type stars (Kilian, Montenbruck, & Nissen 1994), solar-type stars (Edvardsson et al. 1993) and interstellar medium studies (Meyer, Jura, & Cardelli 1998).

Note that this fitting procedure relied on results generated by the light and radial velocity curve analyses described below, while these other analyses rely (albeit very weakly) on the T_{eff} 's determined here. We thus performed these three analyses in an iterative fashion until a self-consistent set of parameters resulted.

4. Modeling the Light Curves

The light curves were solved using an improved version of the Wilson & Devinney (1971; hereafter WD) program (Milone, Stagg, & Kurucz 1992; Milone et al. 1994) that includes Kurucz *ATLAS9* atmosphere models for the computation of the stellar radiative parameters. A detached configuration (as suggested by the eccentric orbit) with coupling between luminosity and temperature was chosen when running the solutions. Both reflection and proximity effects (i.e., tidal distortion) were taken into account, because the light curves clearly show their significance. The bolometric albedo and the gravity brightening coefficients were set to a value of 1.0 as usually adopted for the radiative envelopes of these early-type stars. The mass ratio ($q \equiv M_{\text{S}}/M_{\text{P}}$) was fixed to the spectroscopic value of $q = 0.626$ and the temperature of the primary star was set to 21 350 K. Finally, pseudo-synchronization (synchronization at periastron) was assumed for both components (see Sect. 7).

All three *UBV* light curves were solved simultaneously to achieve a single, mutually consistent, solution. In this simultaneous solution, the relative weight of each curve, which has significant importance, was set according to the r.m.s. residual of the comparison—check star sets (i.e., 0.015, 0.006, and 0.006 for *UBV*, respectively). The free parameters in the light curve fitting were: the eccentricity (e), the longitude of the periastron (ω), the phase offset (ϕ_0), the orbital inclination (i), the temperature of the secondary (T_{S}), the gravitational potentials (Ω_{P} and Ω_{S}), and the luminosity of the primary (L_{P}). Depending on the initial conditions, two different sets of parameters providing good fits to the observations were found. There is not sufficient information in the light or radial velocity curves to discriminate between these two possible solutions, and additional data sources have to be considered to break the

degeneracy. Since the luminosity ratio between the components predicted by the two solutions is very different ($L_{\text{S}}/L_{\text{P}} \approx 0.05$ and $L_{\text{S}}/L_{\text{P}} \approx 0.5$), the spectroscopic light ratio ($L_{\text{S}}/L_{\text{P}} \approx 0.05$, from Paper I) was used to confirm the first solution as the physically preferable one.

An automatic procedure based on MIDAS scripts and FORTRAN programs was employed to execute the WD code. At each iteration, the differential corrections were applied to the input parameters to build the new set of parameters for the next iteration. The result was carefully checked in order to avoid possible unphysical situations (e.g., Roche lobe filling in detached configuration). A solution was defined as the set of parameters for which the differential corrections suggested by the WD code were smaller than the standard errors during three consecutive iterations. However, when a solution was found, the program did not stop. Instead, it was kept running for a given number of iterations, 100 in our case. This was done to test the stability of the solutions, to evaluate their scatter, and to check for possible spurious solutions. For V380 Cyg, the program rapidly converged to a very stable minimum and 47 individual solutions resulted from the 100 iterations. A summary of the best-fitting parameters to the light curve is presented in Table 3.

We also considered – and ultimately rejected – the possibility of a third light contribution to the system. When searching both the SIMBAD database and the Tycho catalogue (ESA 1997) no objects were found within a radius of 1 arcminute centered at the position of V380 Cyg. The system was observed by the Hipparcos mission and there is no indication of visual duplicity down to the spatial and intensity resolution of the satellite ($\rho \approx 0.1 - 0.15$ mas and $\Delta\text{mag} \approx 3.5 - 4$). Moreover, no evidence of stationary spectral lines belonging to a third component are observed in the high S/N spectra used for the spectroscopic study. Since the contribution of the secondary component (whose lines are seen in the spectra) to the total flux of the system in the considered wavelengths is only about 6 percent, we therefore conclude that any third light can be safely neglected.

Additional WD runs were performed starting from the same initial conditions but fixing T_{P} to its proper value $\pm 1\sigma$. This showed that our results from the light curve solution are insensitive

to temperature variations within this range.

A remark should be made at this point concerning the physical meaning of the primary and the secondary eclipses. Since the massive and larger component is also somewhat hotter (and so it has slightly higher surface flux), one would therefore expect the primary (and deeper) eclipse to be a transit of the smaller star in front of the bigger one. However, this is not the case for V380 Cyg, and the primary eclipse turns out to be an occultation of the smaller and cooler component. Such a behavior can be explained in terms of the eccentric orbit and the variations induced by the proximity effects, which can be seen clearly as an out-of-eclipse wave-like variation in Figure 1. Indeed, eccentricity-induced proximity effects produce minimum flux near the phase of the transit, making it the primary eclipse.

The uncertainties in the parameters presented in Table 3 were carefully evaluated by means of two different approaches. On the one hand, the WD program provides the standard error associated with each adjusted parameter. On the other hand, the error can also be estimated as the r.m.s. scatter of *all* the parameter sets corresponding to the iterations between the first solution and the last iteration (about 100). This is, in general, larger than the r.m.s. scatter of the solutions alone, i.e., those that fulfill the criterion previously described. We conservatively adopted the uncertainty as twice whichever of the two error estimates was the largest. The r.m.s. scatters of the residuals in the light curve fit are 0.011 ($n = 264$), 0.006 ($n = 303$) and 0.005 mag ($n = 303$) for U , B , and V , respectively. Figure 1 shows the light curve fits to the observed U , B , and V differential photometry and the corresponding residuals, where no systematic trends are observed. A 3D diagram of V380 Cyg (drawn to scale) is shown in Figure 3, where the tidal deformation of the larger primary component near periastron becomes evident. As shown, the components are nearly spherical in shape at apastron.

The results of the light curve fitting were combined with the velocity semi-amplitudes from the spectroscopic analysis (Paper I) and the UV/optical spectrophotometry study to obtain the absolute dimensions and radiative parameters listed in Table 4. The most recently published complete light curve study dates back to Hill &

Batten (1984). These authors used the LIGHT program to analyze four light curves from various authors and with different qualities. In general, they determined a fractional radius for the primary component that is significantly larger than our value, and for the secondary component this situation is reversed but the difference is much smaller. The reason for such a discrepancy probably originates in the model used in their light curve solution, since the tidal distortion of the primary component is strong and also varies due to the eccentric orbit. In this sense, WD relies on a much more physically rigorous model than LIGHT and thus, our parameters ought to be preferred. Moreover, the fractional radius of the primary component is very well constrained from the shape of the out-of-eclipse curve near periastron (0°15), a region which is not well covered in the light curves analyzed by Hill & Batten (1984). Finally, these authors adopt an effective temperature for the primary component (24 500 K), based on Johnson photometry, which is clearly inconsistent with our detailed analysis. However, their temperature ratio is in good agreement with our result.

An inspection of the masses and radii obtained reveals a binary system composed of two massive stars with rather different physical properties: the more massive primary has evolved beyond the main sequence whereas the lower-mass secondary star is still near to the zero-age main sequence (ZAMS). This situation makes V380 Cyg an extremely important astrophysical tool since it allows the stellar internal structure to be probed during a fast-evolving stage. Our determinations of masses and radii have accuracies of about 4 percent and 2 percent, respectively. This is not as good Andersen (1991) suggests is required for a critical evaluation of stellar evolutionary models. However, because of the short evolutionary timescales of the primary component of V380 Cyg and the strong dependence on the convection parameters, this level of accuracy does allow for important tests of the models, as we will show in §6.

5. Times of Minima and Apsidal Motion Study

V380 Cyg is a challenging system from the viewpoint of times of minima determinations:

both eclipses have long durations (more than 24 hours), they have nearly-flat bottoms, and their shape is perturbed by the wave-like variation seen in the light curves. Therefore, the calculation of the exact time of central-eclipse is not straightforward. Because complete coverage of one eclipse event is not possible during a single night, we decided to combine those observations corresponding to a similar epoch into a light curve and derive the times of the eclipses from comparison with the best available synthetic model. In our particular case, the most natural way of performing such operation is by considering the APT-Phoenix10 and the FCC 0.8-m APT data separately. The periods span about 1 and 2.5 years and have around 100 and 200 measurements per filter, respectively. An additional epoch was retrieved from observations carried out during 1977/78 by Dorren & Guinan (unpublished) at Pahlavi Observatory (Shiraz, Iran). The exact time of minimum determination was then done by fitting synthetic light curves computed with all the parameters listed in Table 3 to the actual observations at three different epochs. The resulting eclipse times are presented in Table 5. In addition, Table 5 lists the eclipse timings from Kron (1935), Semeniuk (1968), and Battistini et al. (1974). The mean HJD of each data set was adopted as the reference epoch. The secondary eclipse published by Semeniuk (1968) was given a much lower weight in the calculations because of the poor coverage of the eclipses and thus the high uncertainty in the time determination.

The eclipse timings listed in Table 5 allow the determination of linear ephemerides independently for primary and secondary eclipses with the following results (numbers between parentheses indicate errors in the last digits and E is the number of cycles):

$$\begin{aligned} T_{\text{MinI}} &= \text{HJD}2441256.544(6) + 12.425719(14) E \\ T_{\text{MinII}} &= \text{HJD}2441261.625(5) + 12.425501(7) E \end{aligned}$$

The difference in the apparent periods is of course a clear indication of the presence of a significant apsidal motion. The complete determination of the apsidal motion rate of V380 Cyg was accomplished in two steps. First, we computed the corresponding time differences $T_{\text{MinII}} - T_{\text{MinI}}$ for each epoch and a linear least-squares fit to the data

clearly showed the presence of a temporal decrement of 1.74×10^{-5} . The observations of Semeniuk (1968) were not used because of the previously mentioned lower accuracy. The result of the linear fit is shown in Figure 4, where the value of Semeniuk's measurement is plotted with an open circle. The measured slope corresponds to an apsidal motion rate of 0.0084 degrees per cycle, or a period of $U = 1460$ years, when an orbital eccentricity of 0.234, an inclination of 82.4 degrees, and a reference longitude of periastron of $\omega_0 = 128$ degrees (representative of the average epoch) are adopted. In computing the apsidal motion rate, terms no higher than e^2 were used in the relevant equations. The slope determination appears to depend critically on Kron's (1935) early data point. However, when this measure is excluded, the resulting slope is still very similar (1.68×10^{-5}) and within the expected uncertainties.

As a second step, because of the relatively large orbital eccentricity, the method described by Giménez & García-Pelayo (1983), with equations revised by Giménez & Bastero (1995), was used for a more accurate calculation of the apsidal motion rate. When adopting the orbital inclination (82.4 ± 0.2 deg) and the eccentricity (0.234 ± 0.008) as derived from the light curve analysis (see Table 3), we obtained an apsidal motion rate of 0.0083 ± 0.0006 degrees per cycle, equivalent to $\dot{\omega}_{\text{obs}} = 24.0 \pm 1.8$ degrees per 100 years or an apsidal motion period of $U = 1490 \pm 120$ years. These values are in excellent agreement with previous determinations and the position of the periastron predicted with these elements for the epoch of the radial velocity curve of Paper I, HJD 2449500, is $\omega = 132.4 \pm 1.5$ degrees also in excellent agreement with that analysis ($\omega = 133.2 \pm 3.2$).

6. Evolutionary Model Study

Stellar evolutionary theory provides a description of the interior structure and the observable properties of a star of given initial mass and chemical composition as a function of age. Significant progress has been made in recent years in understanding the physical processes that govern the structure and evolution of stars, including the computation of accurate nuclear reaction rates, neutrino emission rates, and atmospheric opacities.

Modeling of the convective energy transport mechanism is probably one of the major deficiencies of the current stellar structure and evolution models (see Giménez, Guinan, & Montesinos 1999 and references therein). Because of the extreme mathematical complexity of an accurate treatment, convection is still described through a very simplified and phenomenological theory: the mixing length theory (MLT). When comparing the predictions of the models for stars with convective nuclei, an extra amount of convection (overshooting) is needed to reproduce the observed properties. The overshooting parameter (α_{ov}), i.e., the size in pressure-scale height of the over-extension of the convective nucleus, cannot be theoretically computed and thus needs to be determined from observations. The significance of overshooting is probably one of the largest uncertainties in MLT, as well as the possible dependence of this parameter on mass, evolution or chemical composition. Some attempts (Canuto & Mazzitelli 1991, 1992; Canuto 1999) have been directed towards the development of an essentially parameter-free convection model, but the MLT is still being widely used with fairly good results in most applications.

The eclipsing binaries are powerful tools for testing stellar structure and evolution models, since the fundamental properties of the components (masses, radii, luminosities, etc.) can be accurately determined from observations. Several studies testing the significance of the convective overshooting in the stellar nucleus using eclipsing binary data (Andersen, Nordström, & Clausen 1990; Pols et al. 1997; Ribas et al. 1999) have been published. Although these studies clearly show an improvement when overshooting is included, more quantitative conclusions are difficult to access. This is primarily because the effects of overshooting are only observationally relevant for evolved stages, especially beyond the TAMS. However, no evolved early-type detached eclipsing binaries with accurate determination of absolute dimensions were available to date because of observational selection effects. V380 Cyg is in this sense an important and unique system.

Evolutionary tracks (specifically generated for V380 Cyg) for three different overshooting parameters ($\alpha_{\text{ov}} = 0.2$, 0.4, and 0.6) were kindly provided by A. Claret, for the comparison of the observed stellar properties with the theoretical pre-

dictions. The input physics for these models is identical (except for the enhanced mixing) to that described in Claret (1995), i.e., OPAL opacities, mass loss beyond $10 M_{\odot}$, mixing length parameter $\alpha_p = 1.52$, modern equations of state, extensive nuclear network, etc. The initial masses of the evolutionary tracks were selected so that they would agree with the observed masses of the components at their current evolution stage. A metal abundance of $Z = 0.012$ was adopted as discussed in §3. The helium abundance (Y) that yields the best match to the observed properties of the essentially unevolved secondary component (not affected by the value of the overshooting parameter, see below) was found to be $Y = 0.26 \pm 0.02$. This value is in good agreement with that expected from the metal abundance of V380 Cyg and an average helium-to-metal enrichment law (see Ribas et al. 2000a). A $\log T_{\text{eff}} - \log g$ plot showing the system components and the tracks computed for the adopted chemical composition is presented in Figure 5.

The effect of adopting different values of the overshooting parameter in the early post-ZAMS evolutionary stage of the secondary component is very small. Therefore, its observed properties can be well reproduced by models with wide ranges of convective overshooting. The evolved primary component, however, with $\log g = 3.15$, presents a quite different situation. This star provides an excellent test of convective overshooting. Indeed, the evolutionary track with $\alpha_{\text{ov}} = 0.2$ predicts an effective temperature for the surface gravity of the primary component that is ~ 3000 K ($\sim 7\sigma$) lower than the observed value. Even with $\alpha_{\text{ov}} = 0.4$, the star is predicted to have an effective temperature 2000 K lower than observed. A value of $\alpha_{\text{ov}} = 0.6$ is required to achieve consistency between model predictions and observations, as shown in Figure 5. In this case, the primary component is predicted to be close to the phase of hydrogen shell ignition.

Although not explicitly shown in Figure 5 for the sake of clarity, evolutionary tracks for the observed mass plus and minus 1σ were also available. The $M + 1\sigma$ model for the primary component yields effective temperatures at a given $\log g$ only about 0.009 dex (≈ 500 K) larger than the model for the observed mass. Therefore, even when considering the error bars, the location of the primary component is not compatible with evolutionary

tracks including mild overshooting. A range of overshooting parameters within $\alpha_{\text{ov}} \approx 0.6 \pm 0.1$ is possible when all the observational errors (mass, $\log g$, chemical composition, temperature ratio, etc) are taken into account in the analysis.

Even though the effective temperature is a well-determined quantity in our analysis, it might still be affected by systematics in the model atmosphere fluxes or in the IUE observations. However, our result favoring a large amount of convective core overshooting is immune to any of these effects, because the temperature ratio of the components is accurately determined from the light curve analysis. The good agreement obtained for the secondary component excludes the possibility of resorting to a different value of Y or an error in the zero-point of the temperature scale for explaining the temperature difference. The conclusion of the analysis is based on the tightly-constrained *relative* location of the components in the $\log g - \log T_{\text{eff}}$ diagram (i.e., effective temperature ratio) rather than on the *absolute* value adopted for the effective temperatures.

It is important to note that in a detached system such as V380 Cyg the ages predicted by the models for the two components should agree. This restriction is not very critical for V380 Cyg, however, because the secondary component is close to the ZAMS and, since the observational errors in both the mass and the radius is of the order of 2-3 percent, a wide age range is compatible with the stellar parameters. This is shown in Table 6, where the model predictions (and the errors) are given for the three overshooting values considered. The age, effective temperature, and surface gravity for the primary component are presented in the table. Also included is the age of the secondary component. These parameters were interpolated in the computed tracks at the observed values of $\log g$ for both components. The evolutionary ages for the primary and secondary components are identical within the errors and no significant age-dependent variations are apparent for the various values of the overshooting parameter. Therefore, the coeval criterion for the stars does not favor any particular overshooting parameter but it confirms the good agreement between observed and model predicted physical properties. The age of the system was found to be $\tau = 25.5 \pm 1.5$ Myr when the best-fitting $\alpha_{\text{ov}} \approx 0.6$ was adopted.

A detailed analysis was also carried out with evolutionary tracks of solar metal content ($Z = 0.02$, $Y = 0.28$). From the locations of the stars in the $\log g - \log T_{\text{eff}}$ we found that $\alpha_{\text{ov}} \approx 0.6$ still clearly yields the best fit, although the components are not compatible with coeval evolution (a small age differential of ~ 3 Myr between the components becomes evident).

It has been suggested that the effects of rotation on the structure and evolution of massive stars could mimic those of overshooting. We used evolutionary tracks for V380 Cyg provided by A. Claret (the input physics and approximations are described in detail in Claret 1999) to explore this possibility. Models that include rotation do not show significant differences in the $\log T_{\text{eff}} - \log g$ diagram when compared to the non-rotating models, especially in the evolved stages (a similar conclusion was reached by Deupree 1998). Thus, it appears that this effect cannot mitigate the relatively high value of the overshooting parameter found here.

In practice, the inclusion of rotation in the models only has significant effect when the rotational velocity of the star is fast and approaches the critical value (break up). However, V380 Cyg is a slow rotator ($P \approx 12$ days). The initially faster-rotating eclipsing binary components are braked by tidal effects until they become synchronized with the orbital period. Because the latter is usually quite long for detached massive or intermediate-mass systems, the components spin more slowly than single stars of the same mass. Therefore, evolutionary models that do not include rotation can more confidently be used in eclipsing binaries with massive components than with more rapidly rotating single stars (in clusters, for example).

The determination of the apsidal motion rate of V380 Cyg permits an independent test of stellar model predictions. The apsidal motion rate of an eccentric binary system can be computed from theory as the sum of the contribution of general relativity (GR) and classical (CL) effects (see e.g., Guinan & Maloney 1985). In a system such as V380 Cyg, with a distorted component, the CL contribution to the apsidal motion is expected to dominate the GR term. The classical apsidal motion rate is a function of the orbital (P, e) and physical ($M_{\text{P,S}}, r_{\text{P,S}}, v_{\text{rotP,S}}$) properties of the sys-

tem, all determined from the analysis of the light and radial velocity curves. But in addition, the classical apsidal motion depends on the internal mass distribution of the stars. A star's internal mass distribution is parameterized in polytropic models by the internal structure constant k_2 . In this theory, k_2 is proportional to the ratio of the mean and the central densities of the star. The values of k_2 can be computed from stellar evolution codes (see Claret & Giménez 1992).

An observed apsidal motion rate of $\dot{\omega}(\text{obs}) = 24.0 \pm 1.8 \text{ }^{\circ}/100 \text{ yr}$ was obtained in §5. For comparison with the model predictions, k_2 can be computed from $\dot{\omega}(\text{obs})$ (after correcting for the general relativistic effect, $\dot{\omega}_{\text{GR}} = 2 \text{ }^{\circ}/100 \text{ yr}$) by using the expressions in Claret & Giménez (1993) and by assuming pseudo-synchronization. Additionally, several studies (e.g., Stothers 1974; Claret & Giménez 1993) indicate that a small correction may be needed to include the effects of stellar rotation in the calculation of k_2 .

Taking these effects into consideration, we computed a systemic mean observational value of $\log \bar{k}_2(\text{obs}) = -2.89 \pm 0.04$. The contribution of the secondary component to the mean internal structure constant is negligible (less than 1 percent) because of its small fractional radius. Thus, we assume $\log k_{2P}(\text{obs}) = -2.89 \pm 0.05$. The specially constructed evolutionary models for V380 Cyg, kindly provided by A. Claret, yield the values listed in Table 6. As can be seen, a value of α_{ov} as large as 0.6 ± 0.1 is clearly needed to fit the observed apsidal motion rate of the system.

It is remarkable that the overshooting parameter of $\alpha_{\text{ov}} \approx 0.6 \pm 0.1$ is supported by two independent approaches, namely the investigation of the apsidal motion and the location of the components in the theoretical H-R diagram. The value indicated is significantly larger than that currently adopted by most theoretical models. Some brief comments on the physical implications of this result are left for §8. In addition, a more extensive study on stellar core convection using all the available data from eclipsing binaries is the subject of a forthcoming paper (Ribas, Jordi, & Giménez 2000b).

7. Tidal Evolution

V380 Cyg has an eccentric orbit and the component stars appear to have rotational velocities synchronized with the orbital velocity at periastron, the so called pseudo-synchronization (see Table 4). Pseudo-synchronization is commonly found in eccentric binary systems because in most cases the circularization timescale is much larger than the synchronization timescale (Claret, Giménez, & Cunha 1995). To compare the observations with the theoretical predictions we employed the tidal evolution formalism of Tassoul (1987, 1988). The expressions used, which were taken from Claret et al. (1995), relate the time variation of the eccentricity (\dot{e}) and the angular rotation of the components ($\dot{\Omega}$) with the orbital and stellar physical properties (mass ratio, orbital period, mass, luminosity, radius and gyration radius). It is important to integrate the differential equation that governs the variation of the eccentricity and the angular velocity with time rather than use a simple timescale calculation. This is especially advisable for evolved systems like V380 Cyg because the components may have undergone large radius and luminosity changes that have an important effect over the circularization and synchronization timescales.

Thus, we integrated the differential equations along evolutionary tracks adopting the observed masses of the V380 Cyg components. In these calculations we assumed a constant orbital period. As boundary conditions, we assumed the eccentricity to be the observed value ($e = 0.234$) at the present age of the system ($\tau = 25.5 \text{ Myr}$), and the angular rotation of the stars to be normalized to unity at the ZAMS. The calculations were made with the evolutionary models at $Z = 0.012$, $Y = 0.26$, and $\alpha_{\text{ov}} = 0.6$. The predictions of theory agree well with a system that has reached synchronization for both components but that has not yet circularized its orbit. These calculations indicate that the primary component reduced the difference between its angular velocity and the pseudo-synchronization angular velocity to ≈ 0.1 percent of the ZAMS value at the early age of $\approx 10 \text{ Myr}$, and the same occurred to the secondary component at an age of $\approx 20 \text{ Myr}$.

From the boundary condition it is inferred that the initial (ZAMS) orbital eccentricity was $e \approx$

0.3. A comparison of this initial value with the current observed one indicates a net decrease of $\Delta e \approx 0.07$ in about 25 Myr. The theory also predicts that circularization should occur on a relatively short timescale of $\approx 1.5 \times 10^4$ yr when the radius of the primary star rapidly increases shortly before the initiation of core helium burning. The instantaneous (i.e., with the current parameters) circularization timescale is $\approx 10^8$ yr, much larger than the value computed from the integration of the differential equation because the primary component is located in a very fast evolving stage. Although tidal evolution theory predicts orbital circularization for V380 Cyg in 1.5×10^4 yr, the Roche lobe constraints are not included in the modeling. If these are included, the primary star should fill its Roche lobe in about 10^4 yr. This results in Roche lobe overflow and the initiation of mass transfer. Once V380 Cyg reaches the semi-detached stage, the binary should circularize very rapidly due to strong tidal interactions and friction.

8. Conclusions

This study complements the spectroscopic investigation of V380 Cyg published in Paper I. New differential photometry has been collected in two different epochs, resulting in about 300 observations in each of the *UBV* bandpasses. The photometry has been modeled using an improved version of the Wilson-Devinney program that includes recent model atmospheres. The best fit to the light curves was achieved for the stellar and orbital properties listed in Table 3. The effective temperatures of the stars were determined using UV spectrophotometry and optical photometry. Also, four new eclipse timings were added to the published ones and a complete re-evaluation of the apsidal motion rate of V380 Cyg was carried out.

The determined physical properties (Table 4) of the V380 Cyg components were compared with evolutionary models (with the same input physics as in Claret 1995) computed for the observed masses, and with different values of convective overshoot ($\alpha_{\text{ov}} = 0.2, 0.4$, and 0.6). The fractional abundances of metals and helium were estimated to be $Z = 0.012 \pm 0.003$ (from UV/optical spectrophotometry) and $Y = 0.26 \pm 0.02$ (from evolutionary model fit to the secondary component)

respectively. The best agreement was found for an overshooting parameter of $\alpha_{\text{ov}} \approx 0.6$, for which the primary component is predicted to be located near the blue point of the MS hook. The excellent agreement obtained for the secondary component excludes the possibility of resorting to a different Y value or an error in the temperature scale zero point for explaining the location of the primary component, because the temperature ratio of the components is well-constrained from the light curve analysis. The apsidal motion study of V380 Cyg also indicates that a value of $\alpha_{\text{ov}} \approx 0.6$ is necessary to fit the observed apsidal motion rate of the system. The study of the locations of the components in the $\log g - \log T_{\text{eff}}$ diagram and the internal structure (from apsidal motion) lead to mutually consistent results. However, we caution that the relatively large value of overshooting should be restricted to the mass, evolutionary stage, and chemical composition of the primary component of V380 Cyg.

Our convective overshooting result has a more profound implication than merely providing a better fit to the V380 Cyg data. We have shown that the observed physical properties of V380 Cyg cannot be described by evolutionary models with the most commonly used physical ingredients (including mild overshooting). The physical difference between these standard models and our better-fitting models (with enhanced convective overshooting) is that the latter have larger convective cores. Thus, our more general conclusion is that massive stars have larger convective cores and, therefore, are more centrally condensed than predicted by standard theory. Note that convective overshooting is not the only physical process that might produce such a result. Further increases in the opacity (as it was demonstrated when substituting the LAOL by the newer OPAL opacity tables), diffusive mixing, turbulence or other mechanisms may certainly lead to stellar models with larger and denser convective cores, relaxing the need for our large overshooting parameter. In the meantime, with the current physical ingredients, our results indicate that models should consider a moderate amount of convective overshooting for matching the observed properties of real massive stars.

An investigation of the tidal evolution of V380 Cyg was also carried out. The numeri-

cal integrations of the relevant differential equations indicate a binary system with components in an eccentric orbit that have reached pseudosynchronism. From the theory of Tassoul (1987, 1988), it appears that the orbit circularization should occur on a timescale of 10^4 years. This is on the same timescale as it takes the primary component to fill its Roche lobe and start mass transfer.

This paper clearly demonstrates the importance of specific eclipsing binaries as “astrophysical laboratories”. In the present case of V380 Cyg, fundamental problems of stellar structure and evolution are addressed. Early-type massive systems with at least one evolved component constitute a very important source of observational data for testing stellar structure and core convection. Such systems are scarce (due to strong observational selection effects) and gathering the required photometric and spectroscopic data is not easy (because of the typically long orbital periods – 10 days or more). The relative faintness of the secondary component also presents difficulties in the spectroscopic aspects of the problem. In spite of the observational challenges, these systems (although rare) have proved to be crucial tools and their study should be a priority in stellar astrophysics.

Some examples of early-type eclipsing binaries suitable for testing core convection are: V1756 Cyg, V453 Cyg and V346 Cen (see Ribas et al. 1999). V1765 Cyg has a very massive and evolved component, already in the supergiant stage. V453 Cyg and V346 Cen have primary components of similar mass to that of V380 Cyg but appear to be at a less evolved stage ($\log g \approx 3.8$). Other suitable binaries for testing models are those belonging to the ζ -Aur class of eclipsing binaries (Schröder, Pols, & Eggleton 1997). These are systems with at least one evolved member in the core helium burning or in the supergiant stage. The long periods (hundreds or even thousands of days) make the observations challenging. Hopefully, there will be many more potentially interesting systems to study. The long term monitoring programs associated with (future) space missions and the ground-based systematic surveys (e.g., the Sloan Digital Survey and the OGLE experiment towards the Galactic Bulge) are expected to yield valuable results, both from the detection point of view and from the densely-covered light curves

that they will provide. Finally, extensive photometry of extragalactic eclipsing binaries (in LMC, SMC, and M31) are becoming available as a result of several microlensing (Grison et al. 1995; Alcock et al. 1997; Udalski et al. 1998) and variable star (Kaluzny et al. 1998, 1999; Stanek et al. 1998, 1999) surveys. Such a wealth of data guarantees a nearly inexhaustible source of eclipsing systems meeting the demanding requirements for critical model analysis, not only for solar-type abundances but also for other chemical compositions.

This paper is dedicated to the memory of Dr. Daniel M. Popper who died last September before this work could be completed. We are grateful for his inspiration and for his major contributions to eclipsing binaries. Dr. Antonio Claret is gratefully thanked for computing specific evolutionary tracks for this study. We also wish to thank the contributions of Bryan Deeney and Dr. David H. Bradstreet for help during the early stages of the project. The referee, Dr. Andy Odell, is thanked for a number of important comments and suggestions that led to the improvement of the paper. This work was supported by NASA grant NAG5-2160 and NSF/RUI grants AST 93-15365 and AST 95-28506. I. R. acknowledges support from the predoctoral grant (ref. FI-PG/95-1111) and the postdoctoral Fulbright fellowship by the Catalan Regional Government (CIRIT). E. L. F. acknowledges support from NASA ADP grant NAG5-7117 to Villanova University.

REFERENCES

Alcock, C., Allsman, R. A., Alves, D. et al. 1997, AJ, 114, 326

Andersen, J. 1991, A&AR, 3, 91

Andersen, J., Nordström, B., & Clausen, J. V. 1990, ApJ, 363, L33

Batten, A. H. 1962, Pub. Dom. Astrops. Obs. 12, 91

Battistini, P., Bonifazi, A., & Guarnieri, A. 1974, Ap&SS, 30, 163

Bohlin, R. 1996, AJ, 111, 1743

Böhm-Vitense, E. 1981, Ann. Rev. A&A, 19, 295 (B81)

Canuto, V. M. 1999, *ApJ*, 518, L119

Canuto, V. M., & Mazzitelli, I. 1991, *ApJ*, 370, 295

Canuto, V. M., & Mazzitelli, I. 1992, *ApJ*, 389, 724

Claret, A. 1995, *A&AS*, 109, 441

Claret, A. 1999, *A&A*, 350, 56

Claret, A., & Giménez, A. 1992, *A&AS*, 96, 255

Claret, A., & Giménez, A. 1993, *A&A*, 277, 487

Claret, A., Giménez, A., & Cunha, N. C. S. 1995, *A&A*, 299, 724

Crawford, D. L. 1978, *AJ*, 83, 48

Crawford, D. L., & Mandewewala, N. 1976, *PASP*, 88, 917

Deupree, R. G. 1998, *ApJ*, 499, 340

Edvardsson, B., Andersen, J., Gustafsson, B., Lambert, D. L., Nissen, P. E., & Tomkin, J. 1993, *A&A*, 275, 101

ESA 1997, The Hipparcos and Tycho Catalogues, ESA SP-1200

Figueras, F., Torra, J., & Jordi, C. 1991, *A&AS*, 87, 319

Fitzpatrick, E. L. 1999, *PASP*, 111, 63

Fitzpatrick, E. L., & Massa, D. 1990, *ApJS*, 72, 163

Fitzpatrick, E. L., & Massa, D. 1999, *ApJ*, 525, 1011 (FM99)

Flower, P. J. 1996, *ApJ*, 469, 355 (F96)

Giménez, A. 1984, in *Observational tests of the Stellar Evolution Theory*, eds. A. Maeder & A. Renzini (Dordrecht: Reidel), 419

Giménez, A. 1985, *ApJ*, 297, 405

Giménez, A., & Bastero, M. 1995, *Ap&SS*, 226, 99

Giménez, A., & García-Pelayo, J. M. 1983, *Ap&SS*, 92, 203

Giménez, A., Claret, A., & Guinan, E. F. 1994, presented in the 22nd General Assembly of the IAU (JD 12), The Hague.

Giménez, A., Guinan, E. F., & Montesinos, B. 1999, *Stellar Structure: Theory and Test of Connective Energy Transport*, ASP Conf. Ser., Vol. 173 (San Francisco: ASP)

Grison, P., Beaulieu, J. -P., Pritchard, J. D. et al. 1995, *A&AS*, 109, 447

Guinan, E. F., & Maloney, F. P. 1985, *AJ*, 90, 1519

Guinan, E. F., Fitzpatrick, E. L., DeWarf, L. E., Maloney, F. P., Maurone, P. A., Ribas, I., Giménez, A., Pritchard, J. D., & Bradstreet, D. H. 1998, *ApJ*, 509, L21

Hauck, B., & Mermilliod, M. 1998, *A&AS*, 129, 431

Hill, G., & Batten, A.H. 1984, *A&A*, 141, 39

Jordi, C., Masana, E., Figueras, F., & Torra, J. 1997, *A&AS*, 123, 83

Kaluzny, J., Stanek, K. Z., Krockenberger, M., Sasselov, D. D., Tonry, J. L., & Mateo, M. 1998, *AJ*, 115, 1016

Kaluzny, J., Mochejska, B. J., Stanek, K.Z., Krockenberger, M., Sasselov, D. D., Tonry, J. L., & Mateo, M. 1999, *AJ*, 118, 346

Kilian, J., Montenbruck, O., & Nissen, P. E. 1994, *A&A*, 284, 437

Kopal, Z. 1959, *Close binary systems* (New York: Wiley)

Kron, G. E. 1935, *ApJ*, 82, 225

Kurucz, R. L. 1991, in *Stellar Atmospheres: Beyond Classical Models*, eds. L. Crivellari et al. (Dordrecht: Kluwer), 441

Kurucz, R. L. 1994, CD-ROM No 19

Lyubimkov, L. S., Rachkovskaya, T. M., Rostopchin, S. I., & Tarasov, A. E. 1996, *Astron. Rep.*, 40, 46

Massa, D., & Fitzpatrick, E. L. 2000, *ApJS*, 126, 517

Meyer, D. M., Jura, M., & Cardelli, J. A. 1998, *ApJ*, 493, 222

Milone, E. F., Stagg, C. R., & Kurucz, R. L. 1992, *ApJS*, 79, 123

Milone, E. F., Stagg, C. R., Kallrath, J., & Kurucz, R. L. 1994, *BAAS*, 184, 0605

Nichols, J. S., & Linksy, J. L. 1996, *AJ*, 111, 517

Pols, O. R., Tout, C. A., Schröder, K. -P., Eggleton, P. P., & Manners, J. 1997, *MNRAS*, 289, 869

Popper, D. M. 1980, *Ann. Rev. A&A*, 18, 115 (P80)

Popper, D. M. 1981, *ApJS*, 47, 339

Popper, D. M., & Guinan, E. F. 1998, *PASP*, 110, 572 (Paper I)

Ribas, I., Giménez, A., Jordi, C., Claret, A., & Guinan, E. F. 1999, in *ASP Conf. Ser.* 173, *Stellar Structure: Theory and Test of Connective Energy Transport*, eds. A. Giménez, E. F. Guinan, & B. Montesinos, (San Francisco: ASP), 253

Ribas, I., Jordi, C., Torra, J., & Giménez, A. 2000a, *MNRAS*, 313, 99

Ribas, I., Jordi, C., & Giménez, A. 2000b, *MNRAS*, submitted

Semeniuk, I. 1968, *AcA*, 18, 1

Schmidt-Kaler, T. 1982, *Landolt-Börnstein*, Vol. II, 453

Schröder, K. -P., Pols, O. R., & Eggleton, P. P. 1997, *MNRAS*, 285, 696

Stanek, K. Z., Kaluzny, J., Krockenberger, M., Sasselov, D. D., Tonry, J. L., & Mateo, M. 1998, *AJ*, 115, 1894

Stanek, K. Z., Kaluzny, J., Krockenberger, M., Sasselov, D. D., Tonry, J. L., & Mateo, M. 1999, *AJ*, 117, 2810

Stothers, R. 1974, *ApJ*, 194, 651

Straižys, V. 1992, *Multicolor Stellar Photometry* (Tucson: Pachart Pub. House)

Sūdžius, J., & Bobinas, V. 1992, *Bull. Vilnius Obs.*, 86, 59

Tassoul, J. -L. 1987, *ApJ*, 322, 856

Tassoul, J. -L. 1988, *ApJ*, 324, L71

Udalski, A., Soszyński, I., Szymański, M., Kubiak, M., Pietrzyński, G., Woźniak, P., & Źebruń, K. 1999, *AcA*, 48, 563

Wilson, R. E., & Devinney, E. J. 1971, *ApJ*, 166, 605 (WD)

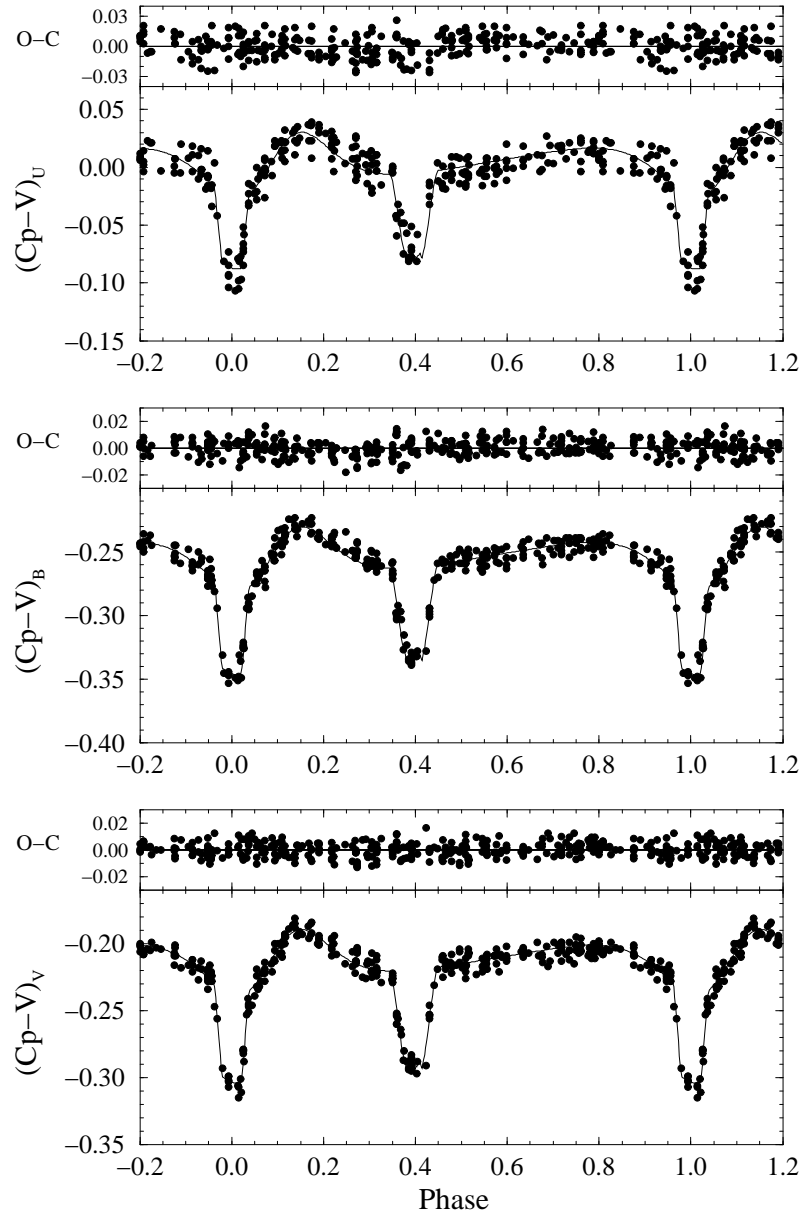


Fig. 1.— Light curve fit to the observed U , B and V Comparison–Variable (Cp–V) differential photometry of V380 Cyg. Also shown are the Observed–Computed (O–C) residuals. The orbital phase was computed according to the following ephemeris: $T_{\text{MinI}} = \text{HJD}2441256.544 + 12.425719 E$.

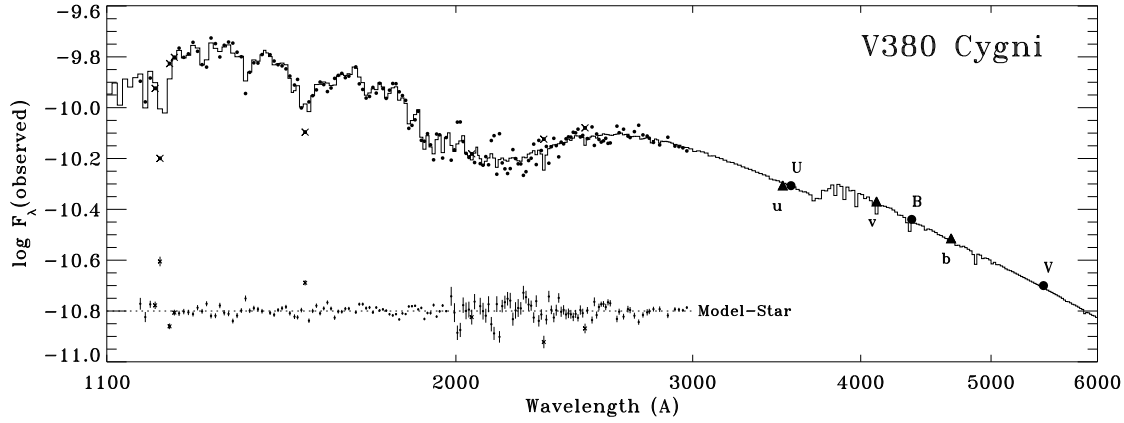


Fig. 2.— Kurucz atmosphere model fit (solid line) to IUE SWP+LWP spectrum (dots) of V380 Cyg. The cross symbols indicate wavelength regions that were not used in the fits chiefly because of the presence of contaminating interstellar medium features. The filled circles and triangles are Johnson and Strömgren fluxes respectively. The residuals of the fit are shown in the lower part of the figure.

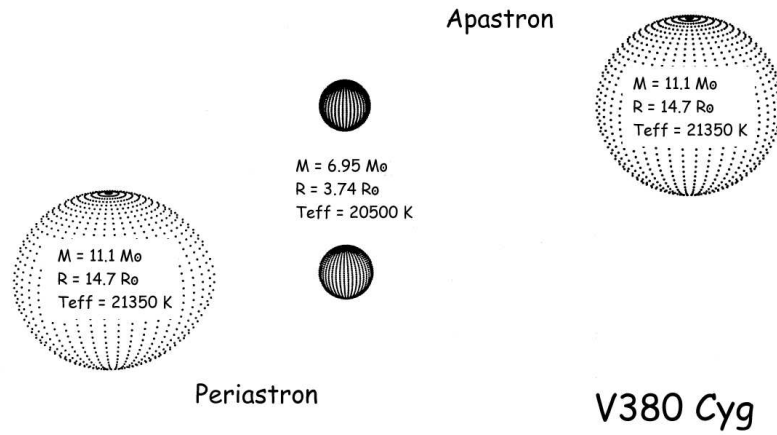


Fig. 3.— 3-D picture of V380 Cyg at periastron and apastron. Notice the slight deformation of the primary component during periastron.

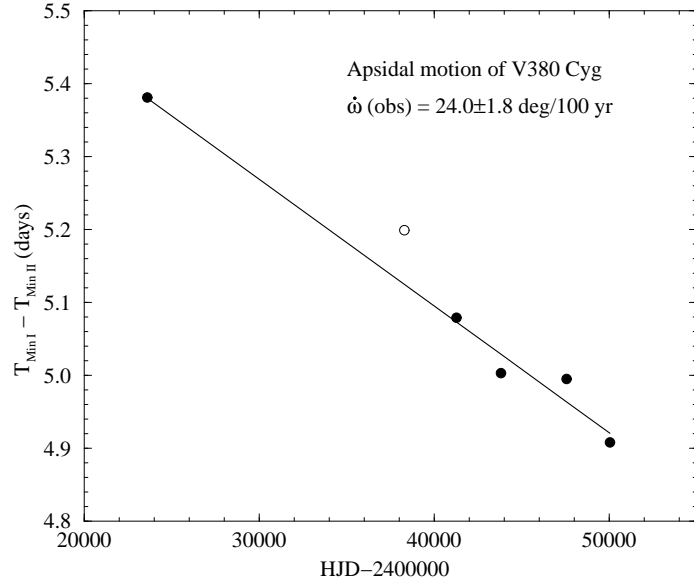


Fig. 4.— Apsidal motion calculation through a linear fit to observed time difference between primary and secondary minima. The slope of the straight line is 1.74×10^{-5} . The individual points have been computed from the times of minima listed in Table 5. Semeniuk's (1968) value is plotted as an open circle and was not used in the fit (see text).

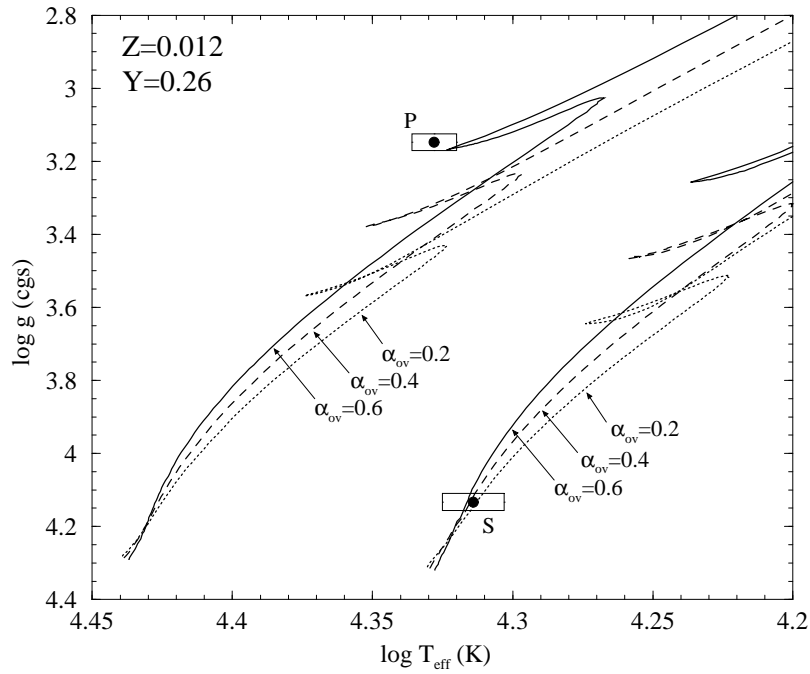


Fig. 5.— $\log g - \log T_{\text{eff}}$ plot of V380 Cyg. Evolutionary tracks for the primary (P) and secondary (S) components computed with $\alpha_{\text{ov}} = 0.2, 0.4$, and 0.6 are shown.

TABLE 1
DIFFERENTIAL PHOTOMETRY FOR V380 CYG IN THE *UBV* BANDPASSES.

| HJD – 2400000 | V – C |
|------------------|--------|------------------|--------|------------------|--------|------------------|--------|------------------|--------|------------------|--------|
| <i>U</i> | | | | | | | | | | | |
| 47415.8013 | -0.004 | 47417.7500 | 0.003 | 47418.7531 | 0.010 | 47419.7573 | 0.107 | 47420.7519 | 0.007 | 47421.7429 | -0.023 |
| 47422.7256 | -0.003 | 47423.7161 | 0.015 | 47424.7076 | 0.081 | 47427.7040 | -0.009 | 47428.7033 | -0.007 | 47429.7106 | 0.004 |
| 47430.7018 | 0.005 | 47431.7010 | 0.042 | 47432.7083 | 0.023 | 47433.7389 | -0.030 | 47436.7233 | 0.048 | 47437.7146 | 0.012 |
| 47441.7282 | -0.013 | 47443.7104 | 0.002 | 47444.7108 | 0.081 | 47459.6380 | -0.017 | 47460.6368 | 0.004 | 47461.6359 | 0.075 |
| 47463.6422 | 0.005 | 47465.6435 | -0.003 | 47466.6301 | -0.015 | 47468.6640 | 0.019 | 47469.6220 | 0.097 | 47470.6211 | -0.021 |
| 47472.6245 | -0.007 | 47475.6085 | 0.005 | 47476.6031 | 0.004 | 47479.5852 | -0.021 | 47481.5778 | 0.081 | 47482.5705 | 0.006 |
| 47483.5706 | -0.035 | 47485.5705 | -0.014 | 47486.5703 | 0.057 | 47494.5554 | 0.058 | 47495.5612 | -0.022 | 47497.5610 | -0.007 |
| 47498.5546 | 0.004 | 47500.5611 | -0.007 | 47502.5549 | 0.004 | 47507.5554 | 0.003 | 47618.0173 | -0.004 | 47619.0159 | 0.016 |
| 47621.0149 | -0.029 | 47622.0135 | -0.012 | 47623.0106 | 0.032 | 47626.9985 | -0.027 | 47629.9922 | -0.010 | 47631.9828 | -0.005 |
| 47632.9770 | -0.037 | 47635.9776 | 0.058 | 47636.9714 | -0.009 | 47641.9575 | -0.020 | 47646.9470 | -0.002 | 47647.9447 | 0.039 |
| 47648.9401 | -0.004 | 47650.9327 | 0.001 | 47651.9321 | -0.019 | 47664.8964 | -0.021 | 47665.8909 | -0.023 | 47668.8804 | 0.010 |
| 47669.9391 | -0.021 | 47670.8765 | -0.020 | 47671.9653 | -0.008 | 47672.8840 | 0.048 | 47673.8940 | -0.001 | 47680.8474 | 0.077 |
| 47683.8784 | -0.017 | 47686.8887 | 0.006 | 47688.8657 | -0.011 | 47689.8647 | -0.013 | 47690.8620 | -0.021 | 47691.8520 | -0.008 |
| 47693.8433 | 0.004 | 47694.8597 | -0.025 | 47695.8595 | -0.022 | 47699.8585 | 0.008 | 47701.8618 | -0.018 | 49864.9458 | -0.023 |
| 49864.9472 | -0.012 | 49864.9482 | -0.022 | 49864.9496 | -0.017 | 49864.9511 | -0.012 | 49866.9329 | -0.014 | 49866.9343 | 0.007 |
| 49866.9353 | 0.008 | 49866.9367 | 0.009 | 49866.9382 | 0.016 | 49867.9052 | 0.052 | 49867.9066 | 0.085 | 49867.9076 | 0.073 |
| 49867.9090 | 0.070 | 49867.9105 | 0.066 | 49868.9408 | -0.023 | 49868.9422 | -0.013 | 49868.9431 | -0.022 | 49868.9446 | -0.008 |
| 49868.9460 | -0.015 | 49869.9487 | -0.030 | 49869.9511 | -0.034 | 49869.9526 | -0.037 | 49870.9376 | -0.027 | 49870.9390 | 0.011 |
| 49870.9400 | -0.018 | 49870.9414 | 0.004 | 49870.9429 | -0.025 | 49871.9413 | 0.005 | 49871.9427 | 0.001 | 49871.9442 | -0.001 |
| 49872.9382 | 0.025 | 49872.9396 | 0.016 | 49872.9406 | 0.013 | 49872.9435 | 0.032 | 49873.9213 | 0.017 | 49873.9223 | 0.014 |
| 49873.9237 | 0.015 | 49873.9252 | 0.004 | 49878.9438 | -0.011 | 49878.9448 | 0.004 | 49878.9477 | -0.018 | 49879.9263 | 0.085 |
| 49879.9277 | 0.104 | 49879.9287 | 0.094 | 49879.9301 | 0.093 | 49879.9316 | 0.073 | 49880.9014 | -0.008 | 49880.9028 | -0.006 |
| 49880.9037 | 0.007 | 49880.9052 | 0.026 | 49880.9067 | 0.001 | 49883.9255 | -0.011 | 49883.9269 | -0.003 | 49883.9279 | 0.003 |
| 49883.9293 | 0.003 | 49883.9308 | -0.011 | 49884.8753 | 0.072 | 49884.8767 | 0.069 | 49884.8777 | 0.051 | 49884.8791 | 0.078 |
| 49884.8806 | 0.078 | 49885.9681 | -0.009 | 49885.9696 | 0.005 | 49885.9705 | -0.001 | 49885.9720 | 0.011 | 49885.9735 | 0.006 |
| 49886.9110 | -0.008 | 49886.9124 | -0.004 | 49886.9134 | 0.008 | 49886.9148 | 0.001 | 49886.9163 | -0.008 | 49887.8951 | -0.018 |
| 49887.8966 | -0.006 | 49887.8976 | -0.006 | 49887.8990 | -0.001 | 49888.9279 | -0.019 | 49888.9293 | -0.014 | 49888.9303 | -0.018 |
| 49888.9332 | -0.016 | 49889.9547 | -0.009 | 49889.9556 | -0.012 | 49889.9571 | -0.006 | 49889.9586 | -0.007 | 49890.8945 | 0.005 |
| 49890.8955 | -0.001 | 49890.8970 | -0.007 | 49890.8984 | -0.007 | 49891.8914 | 0.017 | 49891.8924 | 0.018 | 49891.8938 | 0.034 |
| 49891.8953 | 0.015 | 49892.8909 | 0.033 | 49892.8918 | 0.014 | 49892.8933 | 0.031 | 49892.8947 | 0.023 | 49893.8813 | -0.022 |
| 49893.8827 | -0.005 | 49893.8837 | -0.032 | 49893.8851 | -0.015 | 49893.8866 | -0.022 | 49895.8368 | -0.001 | 49895.8377 | -0.007 |
| 49895.8392 | 0.007 | 49895.8406 | -0.008 | 49896.8944 | 0.042 | 49896.8958 | 0.044 | 49896.8969 | 0.042 | 49896.8983 | 0.059 |
| 49896.8996 | 0.042 | 49898.8474 | -0.009 | 49898.8488 | 0.006 | 49898.8494 | 0.009 | 49898.8512 | 0.007 | 49898.8527 | -0.002 |
| 49899.8733 | -0.020 | 49899.8747 | 0.011 | 49899.8757 | 0.001 | 49899.8771 | -0.005 | 49899.8786 | -0.006 | 49900.8427 | -0.010 |
| 49900.8441 | 0.002 | 49901.8802 | -0.025 | 49901.8816 | -0.023 | 49901.8826 | -0.021 | 49901.8840 | -0.005 | 49901.8855 | 0.004 |
| 50237.9720 | -0.014 | 50237.9734 | -0.002 | 50237.9749 | -0.005 | 50251.9572 | -0.016 | 50251.9587 | 0.006 | 50251.9602 | 0.002 |
| 50252.9618 | 0.079 | 50252.9632 | 0.105 | 50252.9647 | 0.098 | 50253.9527 | -0.023 | 50253.9542 | -0.018 | 50253.9557 | -0.018 |
| 50254.9480 | -0.023 | 50254.9495 | -0.008 | 50254.9510 | -0.039 | 50259.9444 | -0.007 | 50259.9459 | 0.006 | 50259.9473 | -0.001 |
| 50396.5737 | 0.000 | 50396.5752 | 0.014 | 50396.5767 | 0.001 | 50714.6782 | -0.036 | 50714.6797 | -0.036 | 50718.7014 | 0.014 |
| 50718.7028 | -0.008 | 50725.6385 | 0.000 | 50725.6399 | 0.028 | 50725.6415 | 0.021 | 50726.6660 | -0.033 | 50726.6674 | -0.011 |
| 50726.6690 | -0.023 | 50727.6718 | -0.031 | 50727.6733 | -0.025 | 50727.6748 | -0.007 | 50728.6355 | 0.014 | 50728.6370 | -0.011 |
| 50730.6641 | 0.015 | 50730.6656 | 0.014 | 50730.6671 | 0.018 | 50752.5805 | 0.004 | 50752.5820 | -0.026 | 50752.5835 | -0.014 |
| 50753.5971 | 0.018 | 50753.5986 | 0.022 | 50753.6001 | -0.002 | 50754.5965 | 0.079 | 50754.5980 | 0.081 | 50754.5995 | 0.078 |
| 50755.5957 | 0.007 | 50755.5971 | 0.007 | 50755.5987 | 0.019 | 50756.5951 | 0.002 | 50756.5966 | 0.002 | 50756.5981 | 0.016 |
| <i>B</i> | | | | | | | | | | | |
| 47418.7531 | 0.260 | 47419.7573 | 0.349 | 47420.7519 | 0.253 | 47421.7429 | 0.228 | 47422.7256 | 0.250 | 47423.7161 | 0.261 |
| 47424.7076 | 0.332 | 47427.7040 | 0.240 | 47428.7033 | 0.239 | 47429.7106 | 0.236 | 47430.7018 | 0.259 | 47431.7010 | 0.294 |
| 47432.7083 | 0.275 | 47433.7389 | 0.225 | 47436.7233 | 0.303 | 47437.7146 | 0.270 | 47441.7282 | 0.247 | 47443.7104 | 0.255 |
| 47444.7108 | 0.331 | 47459.6380 | 0.240 | 47460.6368 | 0.262 | 47461.6359 | 0.327 | 47463.6422 | 0.258 | 47465.6435 | 0.252 |
| 47466.6301 | 0.241 | 47469.6220 | 0.349 | 47470.6211 | 0.233 | 47472.6245 | 0.249 | 47475.6085 | 0.259 | 47476.6031 | 0.259 |
| 47479.5852 | 0.237 | 47481.5778 | 0.345 | 47482.5705 | 0.266 | 47483.5706 | 0.232 | 47485.5705 | 0.249 | 47486.5703 | 0.323 |
| 47493.5622 | 0.271 | 47494.5554 | 0.326 | 47495.5612 | 0.232 | 47497.5610 | 0.255 | 47498.5546 | 0.259 | 47500.5611 | 0.251 |
| 47502.5549 | 0.244 | 47507.5554 | 0.278 | 47508.5560 | 0.228 | 47618.0173 | 0.281 | 47619.0159 | 0.285 | 47620.0132 | 0.224 |
| 47621.0149 | 0.244 | 47623.0106 | 0.292 | 47624.0024 | 0.272 | 47626.9985 | 0.239 | 47629.9922 | 0.250 | 47631.9828 | 0.251 |
| 47632.9770 | 0.226 | 47633.9797 | 0.234 | 47635.9776 | 0.328 | 47636.9714 | 0.252 | 47646.9470 | 0.260 | 47647.9447 | 0.297 |
| 47648.9401 | 0.259 | 47649.9361 | 0.249 | 47650.9327 | 0.255 | 47651.9321 | 0.248 | 47664.8964 | 0.243 | 47665.8909 | 0.241 |
| 47668.8804 | 0.271 | 47669.9391 | 0.238 | 47670.8765 | 0.243 | 47671.9653 | 0.261 | 47672.8840 | 0.315 | 47673.8940 | 0.259 |
| 47680.8474 | 0.336 | 47683.8784 | 0.249 | 47686.8887 | 0.251 | 47688.8657 | 0.251 | 47689.8647 | 0.250 | 47690.8620 | 0.245 |
| 47691.8520 | 0.248 | 47693.8433 | 0.257 | 47695.8595 | 0.247 | 47697.8955 | 0.261 | 47701.8618 | 0.247 | 47779.7548 | 0.331 |
| 47780.7559 | 0.268 | 47786.7443 | 0.263 | 47788.7233 | 0.241 | 47793.7278 | 0.244 | 47794.7533 | 0.239 | 47797.7467 | 0.328 |
| 47799.7394 | 0.248 | 47800.7425 | 0.243 | 47807.6961 | 0.247 | 47812.6893 | 0.246 | 47813.6851 | 0.241 | 47816.6890 | 0.256 |
| 47817.6812 | 0.294 | 47818.6881 | 0.233 | 47826.6739 | 0.239 | 47833.6399 | 0.257 | 47834.6378 | 0.331 | 47835.6322 | 0.253 |
| 47836.6230 | 0.255 | 47838.6264 | 0.252 | 47840.6143 | 0.245 | 49864.9459 | 0.240 | 49864.9473 | 0.254 | 49864.9483 | 0.247 |
| 49864.9498 | 0.248 | 49864.9512 | 0.243 | 49866.9330 | 0.265 | 49866.9344 | 0.277 | 49866.9354 | 0.268 | 49866.9368 | 0.271 |
| 49866.9383 | 0.269 | 49867.9053 | 0.321 | 49867.9067 | 0.324 | 49867.9077 | 0.326 | 49867.9091 | 0.325 | 49867.9106 | 0.323 |
| 49868.9409 | 0.241 | 49868.9423 | 0.252 | 49868.9433 | 0.245 | 49868.9447 | 0.246 | 49868.9462 | 0.244 | 49868.9474 | 0.235 |
| 49869.9498 | 0.238 | 49869.9528 | 0.240 | 49870.9377 | 0.251 | 49870.9391 | 0.255 | 49870.9401 | 0.253 | 49870.9416 | 0.255 |
| 49870.9430 | 0.253 | 49871.9390 | 0.258 | 49871.9405 | 0.268 | 49871.9414 | 0.267 | 49871.9428 | 0.271 | 49871.9443 | 0.265 |
| 49872.9383 | 0.294 | 49872.9397 | 0.299 | 49872.9408 | 0.294 | 49872.9422 | 0.301 | 49872.9436 | 0.297 | 49873.9200 | 0.254 |
| 49873.9215 | 0.265 | 49873.9224 | 0.259 | 49873.9239 | 0.259 | 49873.9253 | | | | | |

TABLE 1—Continued

| HJD— 2400000 | V—C |
|-----------------|-------|-----------------|-------|-----------------|-------|-----------------|-------|-----------------|-------|-----------------|-------|
| 49901.8842 | 0.249 | 49901.8857 | 0.240 | 50237.9721 | 0.242 | 50237.9735 | 0.250 | 50237.9750 | 0.247 | 50251.9588 | 0.258 |
| 50252.9619 | 0.351 | 50252.9649 | 0.348 | 50253.9529 | 0.239 | 50253.9543 | 0.246 | 50253.9558 | 0.257 | 50254.9481 | 0.228 |
| 50254.9496 | 0.235 | 50254.9511 | 0.223 | 50259.9446 | 0.248 | 50259.9460 | 0.258 | 50259.9475 | 0.250 | 50396.5739 | 0.247 |
| 50396.5753 | 0.253 | 50396.5768 | 0.252 | 50713.6780 | 0.252 | 50713.6794 | 0.257 | 50714.6783 | 0.228 | 50714.6798 | 0.236 |
| 50718.7015 | 0.249 | 50718.7029 | 0.259 | 50718.7044 | 0.248 | 50721.6658 | 0.239 | 50721.6672 | 0.254 | 50721.6688 | 0.243 |
| 50725.6386 | 0.266 | 50725.6401 | 0.275 | 50725.6416 | 0.268 | 50726.6661 | 0.223 | 50726.6676 | 0.232 | 50726.6691 | 0.229 |
| 50727.6719 | 0.238 | 50727.6734 | 0.246 | 50727.6749 | 0.240 | 50728.6342 | 0.256 | 50728.6356 | 0.263 | 50728.6372 | 0.259 |
| 50730.6658 | 0.256 | 50752.5807 | 0.237 | 50752.5821 | 0.244 | 50752.5836 | 0.235 | 50753.5973 | 0.257 | 50753.5987 | 0.259 |
| 50753.6002 | 0.250 | 50754.5966 | 0.334 | 50754.5997 | 0.336 | 50755.5958 | 0.258 | 50755.5973 | 0.264 | 50755.5988 | 0.258 |
| 50756.5952 | 0.252 | 50756.5967 | 0.266 | 50756.5982 | 0.257 | ... | ... | ... | ... | ... | ... |
| <i>V</i> | | | | | | | | | | | |
| 47415.8013 | 0.217 | 47417.7500 | 0.204 | 47418.7531 | 0.227 | 47420.7519 | 0.221 | 47421.7429 | 0.196 | 47422.7256 | 0.215 |
| 47423.7161 | 0.229 | 47424.7076 | 0.297 | 47427.7040 | 0.207 | 47428.7033 | 0.208 | 47429.7106 | 0.208 | 47431.7010 | 0.256 |
| 47432.7083 | 0.239 | 47433.7389 | 0.186 | 47436.7233 | 0.268 | 47441.7282 | 0.209 | 47443.7104 | 0.219 | 47459.6380 | 0.204 |
| 47461.6359 | 0.287 | 47466.6301 | 0.207 | 47469.6220 | 0.311 | 47470.6211 | 0.200 | 47472.6245 | 0.217 | 47475.6085 | 0.218 |
| 47476.6031 | 0.221 | 47479.5852 | 0.205 | 47482.5705 | 0.228 | 47483.5706 | 0.194 | 47485.5705 | 0.221 | 47486.5703 | 0.288 |
| 47493.5622 | 0.234 | 47494.5554 | 0.288 | 47495.5612 | 0.201 | 47497.5610 | 0.222 | 47498.5546 | 0.227 | 47500.5611 | 0.216 |
| 47508.5560 | 0.193 | 47618.0173 | 0.247 | 47619.0159 | 0.246 | 47620.0132 | 0.189 | 47622.0135 | 0.225 | 47623.0106 | 0.256 |
| 47624.0024 | 0.231 | 47626.9985 | 0.202 | 47629.9922 | 0.218 | 47631.9828 | 0.215 | 47632.9770 | 0.187 | 47635.9776 | 0.288 |
| 47636.9714 | 0.216 | 47641.9575 | 0.218 | 47646.9470 | 0.226 | 47647.9447 | 0.264 | 47648.9401 | 0.219 | 47649.9361 | 0.223 |
| 47651.9321 | 0.213 | 47664.8964 | 0.212 | 47665.8909 | 0.204 | 47668.8804 | 0.234 | 47669.9391 | 0.194 | 47670.8765 | 0.197 |
| 47671.9653 | 0.225 | 47672.8840 | 0.280 | 47673.8940 | 0.225 | 47677.8624 | 0.203 | 47680.8474 | 0.301 | 47683.8784 | 0.206 |
| 47686.8887 | 0.216 | 47687.8811 | 0.208 | 47688.8657 | 0.199 | 47689.8647 | 0.215 | 47690.8620 | 0.199 | 47691.8520 | 0.216 |
| 47693.8433 | 0.222 | 47694.8597 | 0.191 | 47695.8595 | 0.208 | 47699.8585 | 0.214 | 47701.8618 | 0.207 | 47779.7548 | 0.293 |
| 47780.7559 | 0.232 | 47788.7323 | 0.199 | 47789.7426 | 0.211 | 47793.7278 | 0.208 | 47794.7533 | 0.200 | 47797.7467 | 0.291 |
| 47799.7394 | 0.210 | 47800.7425 | 0.209 | 47812.6939 | 0.206 | 47813.6851 | 0.201 | 47814.6905 | 0.211 | 47816.6890 | 0.216 |
| 47817.6812 | 0.253 | 47818.6881 | 0.198 | 47826.6739 | 0.207 | 47827.6683 | 0.203 | 47833.6399 | 0.221 | 47834.6378 | 0.293 |
| 47835.6322 | 0.214 | 47836.6230 | 0.219 | 47838.6264 | 0.213 | 47840.6143 | 0.209 | 49864.9461 | 0.200 | 49864.9475 | 0.205 |
| 49864.9485 | 0.202 | 49864.9499 | 0.208 | 49864.9514 | 0.203 | 49866.9332 | 0.226 | 49866.9346 | 0.219 | 49866.9356 | 0.224 |
| 49866.9370 | 0.228 | 49866.9385 | 0.221 | 49867.9054 | 0.282 | 49867.9069 | 0.280 | 49867.9079 | 0.279 | 49867.9093 | 0.280 |
| 49867.9108 | 0.279 | 49868.9410 | 0.201 | 49868.9425 | 0.207 | 49868.9434 | 0.207 | 49868.9448 | 0.210 | 49868.9463 | 0.199 |
| 49869.9476 | 0.194 | 49869.9490 | 0.201 | 49869.9500 | 0.196 | 49869.9514 | 0.200 | 49869.9529 | 0.197 | 49870.9379 | 0.213 |
| 49870.9393 | 0.213 | 49870.9403 | 0.214 | 49870.9417 | 0.215 | 49870.9432 | 0.213 | 49871.9392 | 0.224 | 49871.9406 | 0.229 |
| 49871.9416 | 0.222 | 49871.9430 | 0.226 | 49871.9445 | 0.226 | 49872.9385 | 0.246 | 49872.9399 | 0.256 | 49872.9409 | 0.254 |
| 49872.9423 | 0.253 | 49872.9438 | 0.253 | 49873.9201 | 0.217 | 49873.9216 | 0.226 | 49873.9226 | 0.211 | 49873.9240 | 0.221 |
| 49873.9255 | 0.217 | 49876.8986 | 0.201 | 49876.9000 | 0.201 | 49876.9010 | 0.201 | 49876.9024 | 0.205 | 49876.9039 | 0.195 |
| 49878.9427 | 0.216 | 49878.9441 | 0.221 | 49878.9451 | 0.212 | 49878.9465 | 0.212 | 49878.9480 | 0.216 | 49879.9266 | 0.299 |
| 49879.9280 | 0.303 | 49879.9290 | 0.299 | 49879.9304 | 0.307 | 49879.9319 | 0.302 | 49880.9016 | 0.214 | 49880.9031 | 0.222 |
| 49880.9040 | 0.219 | 49880.9055 | 0.221 | 49880.9069 | 0.228 | 49883.9258 | 0.209 | 49883.9272 | 0.219 | 49883.9282 | 0.218 |
| 49883.9296 | 0.224 | 49883.9311 | 0.212 | 49884.8756 | 0.283 | 49884.8770 | 0.290 | 49884.8780 | 0.286 | 49884.8794 | 0.295 |
| 49884.8809 | 0.285 | 49885.9684 | 0.208 | 49885.9699 | 0.217 | 49885.9708 | 0.215 | 49885.9722 | 0.222 | 49885.9737 | 0.217 |
| 49886.9113 | 0.210 | 49886.9127 | 0.212 | 49886.9137 | 0.209 | 49886.9151 | 0.215 | 49886.9166 | 0.208 | 49887.8954 | 0.206 |
| 49887.8968 | 0.210 | 49887.8978 | 0.204 | 49887.8993 | 0.209 | 49887.9007 | 0.203 | 49888.9282 | 0.199 | 49888.9296 | 0.203 |
| 49888.9306 | 0.205 | 49888.9320 | 0.201 | 49888.9335 | 0.199 | 49889.9353 | 0.198 | 49889.9349 | 0.206 | 49889.9359 | 0.202 |
| 49889.9373 | 0.201 | 49889.9388 | 0.200 | 49890.8934 | 0.209 | 49890.8948 | 0.216 | 49890.8958 | 0.207 | 49890.8972 | 0.203 |
| 49890.8987 | 0.201 | 49891.8902 | 0.222 | 49891.8917 | 0.228 | 49891.8927 | 0.221 | 49891.8941 | 0.228 | 49891.8956 | 0.224 |
| 49892.8897 | 0.241 | 49892.8912 | 0.245 | 49892.8921 | 0.246 | 49892.8935 | 0.251 | 49892.8950 | 0.247 | 49893.8816 | 0.193 |
| 49893.8830 | 0.195 | 49893.8840 | 0.193 | 49893.8854 | 0.200 | 49893.8869 | 0.195 | 49895.8356 | 0.206 | 49895.8370 | 0.207 |
| 49895.8380 | 0.203 | 49895.8394 | 0.204 | 49895.8409 | 0.204 | 49896.8946 | 0.253 | 49896.8961 | 0.260 | 49896.8971 | 0.254 |
| 49896.8986 | 0.260 | 49896.9001 | 0.252 | 49898.8477 | 0.204 | 49898.8491 | 0.209 | 49898.8501 | 0.207 | 49898.8515 | 0.208 |
| 49898.8530 | 0.207 | 49899.8736 | 0.202 | 49899.8750 | 0.213 | 49899.8760 | 0.209 | 49899.8774 | 0.211 | 49899.8789 | 0.211 |
| 49900.8430 | 0.208 | 49900.8444 | 0.210 | 49900.8468 | 0.214 | 49901.8804 | 0.196 | 49901.8819 | 0.205 | 49901.8829 | 0.201 |
| 49901.8843 | 0.206 | 49901.8858 | 0.201 | 50237.9722 | 0.205 | 50237.9737 | 0.207 | 50237.9752 | 0.205 | 50251.9590 | 0.213 |
| 50252.9621 | 0.306 | 50252.9635 | 0.315 | 50252.9650 | 0.307 | 50253.9530 | 0.200 | 50253.9544 | 0.213 | 50253.9559 | 0.205 |
| 50254.9483 | 0.184 | 50254.9497 | 0.192 | 50259.9447 | 0.204 | 50259.9462 | 0.215 | 50259.9476 | 0.209 | 50396.5740 | 0.209 |
| 50396.5754 | 0.209 | 50396.5769 | 0.205 | 50713.6796 | 0.212 | 50714.6785 | 0.185 | 50714.6799 | 0.193 | 50718.7016 | 0.204 |
| 50718.7031 | 0.214 | 50718.7046 | 0.206 | 50721.6659 | 0.199 | 50721.6674 | 0.205 | 50721.6689 | 0.205 | 50725.6388 | 0.219 |
| 50725.6402 | 0.232 | 50725.6417 | 0.224 | 50726.6663 | 0.181 | 50726.6677 | 0.188 | 50726.6693 | 0.185 | 50727.6721 | 0.202 |
| 50727.6735 | 0.209 | 50727.6751 | 0.196 | 50728.6343 | 0.215 | 50728.6358 | 0.215 | 50728.6373 | 0.213 | 50730.6644 | 0.210 |
| 50730.6659 | 0.212 | 50730.6674 | 0.209 | 50752.5823 | 0.200 | 50752.5838 | 0.194 | 50753.5974 | 0.207 | 50753.5989 | 0.220 |
| 50753.6004 | 0.214 | 50754.5968 | 0.294 | 50754.5998 | 0.293 | 50755.5960 | 0.213 | 50755.5974 | 0.219 | 50755.5990 | 0.216 |
| 50756.5954 | 0.211 | 50756.5968 | 0.221 | 50756.5984 | 0.217 | ... | ... | ... | ... | ... | ... |

TABLE 2

PHOTOMETRIC PROPERTIES AND EFFECTIVE TEMPERATURE DETERMINATION OF V380 CYG

| Johnson ^a | Strömgren ^b | Vilnius ^c |
|--|--------------------------------------|--------------------------------------|
| $V = 5.68 \pm 0.02$ | $b - y = 0.031$ | $U - P = 0.20$ |
| $B - V = -0.06 \pm 0.01$ | $m_1 = 0.039$ | $P - Y = 0.37$ |
| $U - B = -0.76 \pm 0.02$ | $c_1 = 0.111$ | $Y - V = 0.22$ |
| | $\beta = 2.587$ | |
| $E(B - V) = 0.18$ | $E(B - V) = 0.19$ | $E(B - V) = 0.23$ |
| $T_{\text{eff}} = 22\,700 \text{ K (F96)}$ | $T_{\text{eff}} = 20\,200 \text{ K}$ | $T_{\text{eff}} = 20\,900 \text{ K}$ |
| $T_{\text{eff}} = 24\,600 \text{ K (P80)}$ | | |
| $T_{\text{eff}} = 23\,100 \text{ K (B81)}$ | | |

^aPhotometry from this work. $E(B - V)$ computed using the intrinsic $(U - B)$ vs $(B - V)$ relation from Schmidt-Kaler 1982 (luminosity class III) and the standard reddening slope of $E(U - B)/E(B - V) = 0.72$. Effective temperatures obtained from T_{eff} vs. $(B - V)_0$ calibrations of Flower 1996 (F96), Popper 1980 (P80) and Böhm-Vitense 1981 (B81).

^bPhotometry from Hauck & Mermilliod 1998. $E(B - V)$ determined from Crawford 1978 — as explained in Figueras, Torra, & Jordi 1991 and Jordi et al. 1997 — and temperature computed by means of the photometric grids of R. Napiwotzki 1998 (private communication), based on Kurucz *ATLAS9* atmosphere models. Coefficients for the color excesses taken from Straižys 1992 and Crawford & Mandewala 1976.

^cPhotometry from Südžiūs et al. 1992. Calibrations in Straižys (1992) used for the calculation of the color excess and the effective temperature.

TABLE 3

RESULTS FROM THE LIGHT CURVE, RADIAL VELOCITY CURVE AND UV/OPTICAL SPECTROPHOTOMETRY ANALYSES.

| Parameter | Value |
|---|--------------------------|
| Light curve | |
| Period (days) | 12.425719 ± 0.000014 |
| Eccentricity | 0.234 ± 0.006 |
| Inclination (deg) | 82.4 ± 0.02 |
| ω (1989.0) (deg) | 132.7 ± 0.3 |
| $\dot{\omega}$ (deg/100 yr) | 24.0 ± 1.8 |
| $\frac{T_{\text{effS}}}{T_{\text{effP}}}$ | 0.96 ± 0.02 |
| $\frac{L_P}{L_S}$ _U | 19.14 ± 0.11 |
| $\frac{L_P}{L_S}$ _B | 17.48 ± 0.08 |
| $\frac{L_P}{L_S}$ _V | 17.31 ± 0.07 |
| r_P | 0.2478 ± 0.0014 |
| r_S | 0.0631 ± 0.0008 |
| Radial velocity curve ^a | |
| K_P (km s ⁻¹) | 94.5 ± 1.5 |
| K_S (km s ⁻¹) | 151.1 ± 3.0 |
| $q \equiv \frac{M_S}{M_P}$ | 0.626 ± 0.041 |
| γ (km s ⁻¹) | 2.4 ± 1.0 |
| a (R _⊕) | 59.2 ± 0.8 |
| UV/Optical Spectrophotometry | |
| T_{effP} (K) | $21\,350 \pm 400$ |
| v_{microP} (km s ⁻¹) | 12 ± 1 |
| v_{microS} (km s ⁻¹) | 0 |
| $[m/H]$ (dex) | -0.44 ± 0.07 |
| $E(B - V)$ (mag) | 0.17 ± 0.02 |
| $\log(R_P^2/d^2)$ | -18.961 ± 0.031 |

^aFrom Paper I.

TABLE 4
PROPERTIES OF THE V380 CYG COMPONENTS.

| | Primary | Secondary |
|---|---------------------|-------------------|
| Spectral Type ^a | B1.5 II-III | B2 V |
| Mass (M_{\odot}) | 11.1 ± 0.5 | 6.95 ± 0.25 |
| Radius (R_{\odot}) | 14.7 ± 0.2 | 3.74 ± 0.07 |
| $\log g$ (cgs) | 3.148 ± 0.023 | 4.133 ± 0.023 |
| T_{eff} (K) | $21\,350 \pm 400$ | $20\,500 \pm 500$ |
| $\log(L/L_{\odot})$ ^b | 4.60 ± 0.03 | 3.35 ± 0.04 |
| M_{bol}^c (mag) | -6.75 ± 0.07 | -3.62 ± 0.10 |
| V^d (mag) | 5.74 ± 0.02 | 8.84 ± 0.02 |
| d^e (pc) | 1000 ± 40 | |
| M_v^f (mag) | -4.79 ± 0.10 | -1.69 ± 0.10 |
| v_{rot}^g (km s $^{-1}$) | 98 ± 4 | 32 ± 6 |
| $v_{\text{rot,p-sync}}^h$ (km s $^{-1}$) | 99 ± 2 | 25 ± 2 |
| $\overline{\rho}$ (g cm $^{-3}$) | 0.0049 ± 0.0003 | 0.187 ± 0.013 |
| ρ_c^i (g cm $^{-3}$) | 3.09 ± 0.24 | 19.6 ± 1.6 |

^aHill & Batten 1984.

^bFrom $L = 4\pi R^2 \sigma T_{\text{eff}}^4$.

^cFrom $\log(L/L_{\odot})$ and adopting $M_{\text{bol}\odot} = 4.75$.

^dComputed from the out-of-eclipse magnitude and $(L_{\text{P}}/L_{\text{S}})|_V$.

^eUsing $\log(R_{\text{P}}^2/d^2)$ from the UV/optical spectrophotometry fit and the observed R_{P} .

^fFrom $M_v = V - 3.1E(B - V) + 5 - 5 \log d$. Note that our values are completely consistent with what is expected for the spectral classification of the components. In addition, $M_{\text{bol}} - M_v$ for both components is in excellent agreement with the bolometric correction calibration of Flower (1996).

^gComputed from Lyubimkov et al. 1996.

^hPseudo-synchronization rotational velocity.

ⁱFollowing Kopal 1959 and using the internal concentration parameters k_2 .

TABLE 5
SUMMARY OF TIME OF MINIMA DETERMINATION FOR V380 CYG.

| HJD | Type ^a | Reference |
|---------------------|-------------------|----------------------------|
| 2423587.184 ± 0.009 | P | Kron 1935 |
| 2423592.565 ± 0.007 | S | Kron 1935 |
| 2438274.372 ± 0.003 | P | Semeniuk 1968 |
| 2438279.571 ± 0.020 | S | Semeniuk 1968 |
| 2441256.541 ± 0.003 | P | Battistini et al. 1974 |
| 2441261.620 ± 0.004 | S | Battistini et al. 1974 |
| 2443791.412 ± 0.010 | P | Dorren & Guinan (unpub.) |
| 2443796.416 ± 0.010 | S | Dorren & Guinan (unpub.) |
| 2447543.936 ± 0.005 | P | This study (APT-Phoenix10) |
| 2447548.931 ± 0.005 | S | This study (APT-Phoenix10) |
| 2450029.125 ± 0.005 | P | This study (FCC 0.8-m APT) |
| 2450034.033 ± 0.005 | S | This study (FCC 0.8-m APT) |

^aP and S stand for primary and secondary minimum, respectively.

TABLE 6
MODEL PREDICTIONS WITH DIFFERENT AMOUNTS OF OVERSHOOTING FOR THE COMPONENTS OF V380 CYG.

| α_{ov} | Primary comp. | | | Secondary comp. | | |
|----------------------|---------------|-----------------------|--------------|-----------------|-----------------------|--------------|
| | Age (Myr) | $\log T_{\text{eff}}$ | $\log k_2$ | Age (Myr) | $\log T_{\text{eff}}$ | $\log k_2$ |
| 0.2 | 20.5 ± 1.5 | 4.267 ± 0.010 | -2.66 ± 0.03 | 20 ± 3 | 4.311 ± 0.009 | -2.10 ± 0.02 |
| 0.4 | 22.9 ± 1.5 | 4.282 ± 0.010 | -2.75 ± 0.03 | 23 ± 3 | 4.313 ± 0.009 | -2.11 ± 0.02 |
| 0.6 | 25.2 ± 1.5 | 4.324 ± 0.010 | -2.91 ± 0.03 | 26 ± 3 | 4.314 ± 0.009 | -2.11 ± 0.02 |